The 32- and 14-Kilodalton Subunits of Replication Protein A Are Responsible for Species-Specific Interactions with Single-Stranded DNA†

Zita A. Sibenaller, Brenda R. Sorensen, and Marc S. Wold*

Department of Biochemistry, University of Iowa College of Medicine, 51 Newton Road, Iowa City, Iowa 52242

Received May 13, 1998; Revised Manuscript Received July 10, 1998

ABSTRACT: Replication protein A (RPA) is a multisubunit single-stranded DNA-binding (ssDNA) protein that is required for cellular DNA metabolism. RPA homologues have been identified in all eukaryotes examined. All homologues are heterotrimeric complexes with subunits of ∼70, ∼32, and ∼14 kDa. While RPA homologues are evolutionarily conserved, they are not functionally equivalent. To gain a better understanding of the functional differences between RPA homologues, we analyzed the DNA-binding parameters of RPA from human cells and the budding yeast *Saccharomyces cerevisiae* (hRPA and scRPA, respectively). Both yeast and human RPA bind ssDNA with high affinity and low cooperativity. However, scRPA has a larger occluded binding site (45 nucleotides versus 34 nucleotides) and a higher affinity for oligothymidine than hRPA. Mutant forms of hRPA and scRPA containing the high-affinity DNA-binding domain from the 70-kDa subunit had nearly identical DNA binding properties. In contrast, subcomplexes of the 32- and 14-kDa subunits from both yeast and human RPA had weak ssDNA binding activity. However, the binding constants for the yeast and human subcomplexes were 3 and greater than 6 orders of magnitude lower than those for the RPA heterotrimer, respectively. We conclude that differences in the activity of the 32- and 14-kDa subunits of RPA are responsible for variations in the ssDNA-binding properties of scRPA and hRPA. These data also indicate that hRPA and scRPA have different modes of binding to ssDNA, which may contribute to the functional disparities between the two proteins.

Replication protein A (RPA)[1] was originally purified as a single-stranded DNA-binding protein essential for SV40 DNA replication (*1*−*3*). Subsequently, RPA was shown to be required for multiple processes in cellular DNA metabolism including DNA replication, DNA repair, and recombination (see ref *4* for general review). RPA may also have roles in the regulation of gene expression and the coordination of the cell cycle (*4*−*7*). Human RPA (hRPA) is a stable, heterotrimeric complex composed of 70-, 32-, and 14-kDa subunits (*2*, *3*). Homologous heterotrimeric single-stranded DNA-binding proteins have been identified in all eukaryotes examined (reviewed in refs *4* and *8*). Several lines of evidence indicate that all of the subunits are required for RPA function: biochemical studies have shown that deletion mutants and subcomplexes of RPA are not active in DNA replication (*4*, *9*), and genetic studies in *Saccharomyces cerevisiae* have shown that all three genes are essential for viability (*10*, *11*). Furthermore, point mutations or other small changes in any of the three genes for RPA can cause defects in DNA metabolism in vivo (*5*, *12*−*18*).

The 70-kDa subunit of RPA (RPA70) has an intrinsic high-affinity ssDNA-binding activity and specifically interacts with multiple other proteins (*4*, *9*, *37*). This subunit has been studied extensively and its structural and functional domains have been mapped. It is composed of an N-terminal domain (residues ∼1−170) that participates in protein−protein interactions, a central DNA binding domain (residues ∼170−450) that can also participate in protein−protein interactions and a C-terminal domain (residues ∼450−616) that is required for interactions with the 32- and 14- kDa subunits of RPA (*9*, *20*−*25*). DNA sequence analysis and structural studies have demonstrated that the central DNA-binding domain is composed of two copies of a ssDNA-binding motif (*15*, *25*). The crystal structure indicates that the DNA binding domain directly interacts with 8 nucleotides of ssDNA (*25*).

Defining the function of the 32- and 14-kDa subunits of RPA (RPA32 and RPA14, respectively) has been more elusive. These subunits form a soluble complex (RPA32·14) that has been implicated in the formation of the RPA complex (*26*, *27*). RPA32 participates in specific protein−protein interactions (*4*, *7*, *28*, *29*) and has been shown to be phosphorylated upon binding to ssDNA (*4*, *6*, *20*, *30*−*33*).

† These studies were supported by Grant GM44721 from the National Institutes of Heath General Medicine Institute. B.R.S. was supported by NIH/National Institute on Aging Grant T32-AG-00214, Interdisciplinary Research Training Program on Aging, University of Iowa. Initial stages of this project were supported by the Roy J. Carver Charitable Trust.

* To whom correspondence should be addressed: Phone (319) 335-6784; Fax (319) 335-9570; Email marc-wold@uiowa.edu.

[1] Abbreviations: RPA, replication protein A; hRPA, human replication protein A holoenzyme; scRPA, *Saccharomyces cerevisiae* replication protein A holoenzyme; hRPA32·14, complex of 32-kDa and 14-kDa subunits of human replication protein A; scRPA32·14, complex of 32-kDa and 14-kDa subunits of *Saccharomyces cerevisiae* replication protein A; RPA70, 70-kDa subunit of replication protein A; RPA32, 32-kDa subunit of replication protein A; RPA14, 14-kDa subunit of replication protein A; ssDNA, single-stranded DNA; DTT, dithiothreitol; GMSA, gel mobility shift assay; SDS−PAGE, sodium dodecyl sulfate−polyacrylamide gel electrophoresis; nt, nucleotide.

S0006-2960(98)01110-6 CCC: $15.00
Published on Web 08/15/1998

Recent studies indicate that phosphorylation modulates RPA−protein interactions (K. A. Braun, unpublished). Thus, RPA32 appears to have a role in regulating RPA function. It was originally proposed, on the basis of sequence homology, that both the 32- and 14-kDa subunits could interact with ssDNA (*15*). While initial studies of an isolated hRPA32·14 subcomplex detected no ssDNA-binding activity (*26*), subsequent studies in several laboratories have shown that RPA32 can interact with ssDNA (*34*−*36*).

All RPA homologues bind with high affinity to ssDNA (*4*) and participate in specific protein−protein interactions (*4*, *37*). However, RPA homologues are not functionally equivalent. The coding sequences of the subunits of human RPA cannot complement a null mutation of the homologous yeast gene (*10*, *11*). In vitro, human, bovine, and *Drosophila melanogaster* RPA can support SV40 DNA replication (*2*, *3*, *38*−*40*), while the homologues from yeast or trypanosomes cannot (*40*−*43*). In addition, the ability to support SV40 replication is highly correlated with the ability of the homologue to participate in specific interactions with SV40 large T antigen and DNA polymerase α (*37*−*40*, *44*, *45*). These data have been interpreted to indicate that species-specific RPA−protein interactions are essential for RPA function in DNA replication; however, the role of these specific interactions in DNA replication is not known (*37*; K. A. Braun, unpublished data).

The binding properties of hRPA and scRPA have been examined in detail (*46*−*49*). Initial analyses showed that both homologues had a much higher affinity for ssDNA than double-stranded DNA and both showed a preference for binding pyrimidine residues (*46*, *50*, *51*). hRPA was shown to have an occluded binding site size of ∼30 nt and bound ssDNA with low cooperativity ($\omega = \sim 10-20$) (*46*−*48*, *52*, *53*). [Similar binding parameters have also been observed for RPA homologues from *D. melanogaster* and *Bos taurus* (*54*−*56*).] In contrast, scRPA was initially shown to have an occluded binding site of 90−100 nt and to bind with very high cooperativity ($\omega = 10^4-10^5$) (*49*). Recently, an independent study reported the occluded binding site of scRPA to be between 20 and 30 nt (*57*).

We have characterized the DNA-binding properties of hRPA and scRPA under uniform conditions. We find that the DNA-binding properties of scRPA are significantly different from those of hRPA: scRPA has an occluded binding site 30% larger and an affinity for oligothymidine 5-fold higher than hRPA. We find no evidence for a 90 nt, highly cooperative binding mode for scRPA. By examining subcomplexes from human and yeast RPA, we show that the 32- and 14-kDa subunits are probably responsible for the differences in binding properties observed between the two RPA homologues. These studies indicate that scRPA and hRPA have different modes of binding to ssDNA and that this may contribute to their differences in function.

EXPERIMENTAL PROCEDURES

Materials. Restriction endonucleases, Vent DNA polymerase, primers used in PCR, and polynucleotide kinase were purchased from New England Biolabs or Life Technologies, Inc. [γ-^{32}P]ATP (>5000 Ci/mmol) was purchased from Amersham. Oligonucleotides were obtained from The Midland Certified Reagent Company or the University of Iowa DNA Core Facility. *Escherichia coli* expression strain BL21 (DE3) cells were from W. Studier (*58*). A 100 mM stock solution of isopropyl β-D-thiogalactopyranoside (IPTG; Research Products International) was used. Buffers used were HI buffer [30 mM HEPES (diluted from a 1 M stock at pH 7.8), 0.25 mM EDTA, 0.5% (w/v) inositol, and 0.01% (v/v) NP40] and filter binding buffer [30 mM HEPES (diluted from a 1 M stock, pH 7.8), 5 mM $MgCl_2$, 100 mM NaCl, 0.5% inositol (w/v), and 1 mM dithiothreitol].

DNA Methods. Restriction endonucleases and Klenow fragment were used according to the manufacturers' recommendations. Oligonucleotides were radiolabeled with [γ-^{32}P]-ATP using polynucleotide kinase (*59*). Polymerase chain reactions (PCR) were performed with Vent DNA polymerase (New England Biolabs) in a DNA thermal cycler (Perkin-Elmer). DNA amplification conditions were 30 cycles of 94 °C for 1 min, 45 °C for 1 min, and 72 °C for 3 min. PCR products and DNA fragments were isolated from 1% TAE−agarose gels with a Geneclean II kit (BIO 101, La Jolla, CA) according to the manufacturer's specifications. Ligation reactions and transformations were according to Ausubel et al. (*59*). Recombinant plasmids were transformed into *E. coli* DH5α cells and isolated by the boiling lysis method (*59*). DNA sequencing was performed on an Applied Biosystems 373A automatic DNA sequencer at the DNA Core Facility at the University of Iowa.

Protein Methods. Protein concentrations were determined by Bradford assay (Bio-Rad) with bovine serum albumin as a standard. Extinction coefficients of purified hRPA (92.2×10^3 M^{-1} cm^{-1}) and scRPA (98.5×10^3 M^{-1} cm^{-1}) were determined using the method of Edelhoch (*60*, *61*). Purity of protein fractions was determined by SDS−PAGE on 8−14% gradient gels as described previously (*26*). Gels were either stained with coomassie blue or with silver nitrate (*59*).

Plasmid Construction. We have described the construction of a plasmid vector containing all three subunits of human RPA previously (*26*). A similar plasmid was made containing the genes for the three subunits of scRPA. pJM114, pJM223, and pJM320, containing the wild-type RFA1, RFA2 (without intron), and RFA3 genes, respectively, were obtained from Dr. Steven Brill (*11*). RFA1 and RFA3 genes were amplified by PCR so that *Nco*I and *Bam*HI or *Bam*HI restriction sites were introduced at the 5′ or 3′ ends of the genes, respectively. The primers used were as follows, with nucleotide base changes introduced indicated by underlines: RFA1 5′ TATGGATCCAAGCCATGGGCAGTGTTCAA 3′; 5′ ACAATCGAATTACCTAGGTTA 3′; RFA3 5′ CAAGGATCCATGGCCAGCGAA 3′; 5′ TACTACTATCATCCTAGGCAG 3′. The RFA1 and RFA 3 gene products were isolated, digested with *Nco*I and *Bam*HI, and individually ligated into pET-11d digested with *Nco*I and *Bam*HI to generate plasmids p11d-scRPA70 and p11d-scRPA14, respectively. p11d-scRPA14 was digested with *Bam*HI and the fragment containing the Shine−Dalgarno sequence and the scRPA14 gene was ligated into pUC18 digested with *Bam*HI to yield pSD-scRPA14. The *Bam*HI fragment of pSD-scRPA14 containing the scRPA14 gene was ligated to pJM223 (pET-11a containing the RFA2 gene) digested with *Bam*HI to produce p11a-RPAsc30/sc14. A *Bgl*II−*Cla*I fragment from p11a-RPAsc30/sc14 containing the genes for the two smaller subunits of scRPA was isolated

and ligated to p11d-scRPA70 digested with *Bam*HI and *Cla*I to generate p11d-tscRPA. This plasmid contained all three genes for the subunits of scRPA under the control of the T7 promoter with each gene having a Shine−Dalgarno sequence upstream of the start codon.

A plasmid capable of expressing the first 442 amino acids of scRPA70 was generated by PCR using the scRPA70 cDNA at a template. The N-terminal primer was the same as described above for scRPA70. Similarly, a C-terminal primer was designed with nucleotide base changes that created two stop codons starting at residue 443 followed by a *Hin*dIII restriction site. The C-terminal primer used to amplify the specific region of scRPA70 is shown below with base changes indicated by underlines: 5′ CTGAAGCTTTCATTATGTTAAGCT 3′. The truncated scRPA70 gene produced by PCR was digested with *Nco*I and *Hin*dIII and ligated to pET-11d vector that had been digested with *Nco*I and *Hin*dIII. The resulting plasmid, plld-RPA70Δ442−623, containing the coding sequence for scRPA70Δ442−623 (scRPA70ΔC442) under the control of the T7 promoter was isolated and confirmed by DNA sequencing.

A plasmid capable of expressing RPA14 and the central domain of hRPA32, residues 43−171, was made. p3d-RPA14/32, which contains the coding sequences for hRPA14 and hRPA32 genes (*26*), was used as a template for a PCR reaction using 5′ AAATCAGGATCCATGGCCCAGCACATTGTG 3′ and 5′ GGGCTGAAGCTTTCATTTGCTTAGTAC 3′ as the N- and C-terminal primers, respectively. This produced a truncated form of hRPA32 containing amino acids 43−171. Base pair changes (indicated by underlines in the primers) in the N-terminal primer created *Bam*HI and *Nco*I restriction sites and an ATG start codon, and changes in the C-terminal primer introduced a stop codon followed by a *Hin*dIII restriction site. The full-length hRPA32 coding sequence was removed from p3d-RPA14/32 by digestion with *Bam*HI and *Hin*dIII, and the *Bam*HI−*Hin*dIII-digested vector was ligated to the PCR amplified RPA32(43−171) fragment that had also been digested with *Bam*HI and *Hin*dIII. The resulting plasmid, p3d-RPA14·32(43−171), contains the hRPA14 and hRPA32(43−171) coding sequences. The sequence of this vector was confirmed by DNA sequencing.

Protein Purification. hRPA, hRPA70ΔC442, and hRPA32·14 were purified as described previously (*21*, *26*).

Purification of scRPA. p11d-tscRPA was transformed into *E. coli* expression strain BL21(DE3) cells (*58*) as described previously (*26*). Recombinant scRPA protein was purified as described previously for hRPA (*26*). All steps were carried out at 4 °C. The soluble fraction (280.6 mg) from 2 L of induced culture was applied to a 50 mL Affi-Gel Blue (Bio-Rad) column that was equilibrated in HI buffer containing 80 mM KCl. The column was washed successively with 150 mL each of HI buffer containing 80 mM KCl, 800 mM KCl, 0.5 M NaSCN, and 1.5 M NaSCN. Partially purified scRPA protein (39.6 mg) eluted in the 1.5 M NaSCN wash. These fractions were pooled and applied to a 10 mL hydroxylapatite (Calbiochem) column that was equilibrated in HI buffer. The hydroxylapatite column was successively washed in HI buffer containing 0, 80, and 500 mM potassium phosphate (pH 7.5). Fractions collected during the 80 mM potassium phosphate wash contained scRPA. These fractions were pooled (6 mg) and applied to a 1 mL Mono-Q (HR5/5) column (Pharmacia) that had been equilibrated in HI buffer containing 100 mM KCl. The column was washed sequentially with 2 mL each of HI buffer containing 100 and 200 mM KCl, respectively, before elution with a 10 mL linear salt gradient from 200 to 400 mM KCl. Two peaks of protein were obtained: purified scRPA32·14 subcomplex eluted at ∼210 mM KCl and purified scRPA heterotrimer eluted at ∼250 mM KCl. Final yields for scRPA and scRPA32·14 are ∼1 mg and ∼0.2 mg/L of culture, respectively. Throughout the purification procedure, the presence of scRPA was monitored by SDS−polyacrylamide gel electrophoresis followed by staining with silver nitrate.

Purification of scRPA70ΔC442. Cells were transformed with p11d-scRPA70Δ442−621, induced, and lysed as described previously (*26*). Purification of recombinant scRPA70ΔC442 was similar to the protocol described for hRPA70ΔC442 (*21*) with the following exceptions. Soluble lysates from 2 L of an induced culture was applied to a 25-mL Affi-Gel Blue (Bio-Rad) column equilibrated with HI buffer containing 80 mM KCl. The column was washed sequentially with 90 mL each of HI buffer containing 80 mM KCl, 800 mM KCl, 0.5 M NaSCN, and 1.5 M NaSCN. Partially purified scRPA70ΔC442 protein eluted in the 1.5 M NaSCN wash. These fractions were pooled and applied to a 7-mL hydroxylapatite (Calbiochem) column that had been equilibrated in HI buffer with 1.5 M NaSCN. The column was washed with HI buffer followed by elution with a 70-mL linear salt gradient from 0 to 250 mM potassium phosphate in HI buffer. Highly purified scRPA70ΔC442 protein eluted as a single peak at ∼200 mM potassium phosphate. This protein migrated as a single band on an SDS−polyacrylamide gel stained with silver nitrate (data not shown).

Purification of hRPA32(43−171)·14. Cells were transformed with p3d-hRPA14·32(43−171), induced, and lysed as described previously (*26*). Protein was monitored by Western blotting. Soluble lysates from 2 L of induced culture (185 mg of total protein) were separated on an Affi-Gel Blue (Bio-Rad) column as described above. The peak of hRPA14·32(43−171) protein (∼38 mg) eluted in the 800 mM KCl wash (60 mL). These fractions were pooled and applied to a 7-mL hydroxylapatite column equilibrated with HI buffer. After the column was washed with 3 column volumes of HI buffer, a 70-mL linear gradient was developed containing 0−250 mM potassium phosphate. A single peak at 75 mM potassium phospate contained partially purified protein (∼15 mg). $(NH_4)_2SO_4$ (2 M) was added to 7 mg of the partially purified protein to give a final concentration of 1.7 M. This protein fraction was applied to a phenyl-Superose HR5/5 column (Pharmacia) that had been equilibrated in 1.7 M $(NH_4)_2SO_4$. The column was washed with 3 column volumes of 1.7 M $(NH_4)_2SO_4$ before a 20 column volume linear gradient from 1.7 to 0 M $(NH_4)_2SO_4$ was developed. The protein eluted at ∼0.1 M $(NH_4)_2SO_4$. These fractions were pooled (1.5 mL) and applied to a Mono-Q HR5/5 column (Pharmacia) that was equilibrated in 50 mM KCl. A single peak of protein corresponding to hRPA32-(core)·14, eluted in the 50 mM KCl wash and contained 0.75 mg of protein.

Analytical Ultracentrifugation. To determine the state of self-association of human and yeast RPA and the mutant scRPA70ΔC442 under low (0.1 M) and high (1.5 M) salt

conditions, sedimentation equilibrium studies were conducted with a Beckman XL-I analytical ultracentrifuge (Beckman Instruments, Inc., Fullerton, CA) at 25 °C with six-channel equilibrium centerpieces following general procedures described by Laue (*62*).

Purified RPA and scRPA70ΔC442 were extensively dialyzed against a 10-fold greater volume of filter binding buffer with either 0.01% Tween 20 or 1.5 M NaCl/0.01% Tween 20. Proteins were then diluted to concentrations between 0.125 and 0.5 mg/mL in the appropriate dialysis buffer prior to ultracentrifugation.

Sedimentation of all samples was monitored by absorbance at 280 nm. Multiple concentrations of each protein were centrifuged at 8000, 10 000, and 14 000 rpm until equilibrium was established (18−24 h.). Baseline absorbance was subsequently determined by meniscus depletion of the sample at 50 000 rpm for 2 h. The reduced apparent molecular mass (σ; *62*) was resolved by fitting the data from all samples globally using nonlinear least-squares analysis (WinNonlin Version 1.03 by Yphantis and Lary; see ref *63*). In fitting the data to a model describing a single ideal species in solution, ln $C_{1,0}$ and σ were allowed to vary and the natural logarithms of the association constants (ln K_2, ln K_3, ln K_4, and ln K_5) were fixed to -1.00×10^4; N_2, N_3, N_4, and N_5 were fixed at 2, 3, 4, and 6, respectively; and B was fixed at 0. Multiple criteria reported by NONLIN (*64*) were used for evaluating goodness-of-fit of the data to the model. These error statistics included (a) the value of the square root of variance, (b) the values of asymmetric 65% confidence intervals, (c) the systematic trends in the distribution of residuals, (d) the magnitude of the span of residuals, and (e) the absolute value of elements of the correlation matrix.

Fluorescence Titrations. Fluorescence studies were performed on an SLM 4800C spectrofluorometer. Forms of RPA were titrated with oligonucleotides as indicated and changes in the intrinsic protein fluorescence were monitored as described previously (*47*, *48*). All assays were carried out in filter binding buffer containing 0.01% Tween 20 and the indicated concentration of NaCl. Protein samples were excited at 292 nm and emission was monitored at 346 nm. Photobleaching under these conditions was less than 2%. The decrease in intrinsic fluorescent signal or quenching was calculated as the absolute change in signal normalized by the initial fluorescence in the absence of DNA and corrected for dilution effects (*65*). The protein concentration of samples used was initially determined by Bradford assay and confirmed by UV spectroscopy. The concentration of active protein was experimentally determined for each reverse titration with a $(dT)_{30}$ substrate, and the percent quenching was plotted versus DNA/RPA ratio (mol/mol) as described previously (*21*). Analysis of equilibrium binding experiments was carried out as described previously (*47*, *48*). Briefly, binding data were fit to the Langmuir equation [converted to a function of total active RPA and total DNA (*47*)] by nonlinear least-squares fitting using KaleidaGraph (Abelbeck Software).

RESULTS

Characterization of Recombinant scRPA. As has been observed previously with several RPA homologues (*15*, *26*, *66*), when the three subunits of scRPA were expressed simultaneously in *E. coli*, a soluble heterotrimeric complex was produced (data not shown). The properties of scRPA during purification were identical to those of hRPA (see Experimental Procedures and ref *26*) with the exception that Mono-Q chromatography yielded two protein peaks. One was heterotrimeric scRPA and the second was a subcomplex of scRPA32·14. Both fractions were homogeneous as determined by SDS−PAGE followed by staining with silver (data not shown). Partial proteolysis of the scRPA complex demonstrated that its protease-sensitive sites and the kinetics of digestion were similar to those of hRPA (data not shown; see also ref *20*). This suggests that the general structures of scRPA and hRPA are similar.

Table 1: Molecular Mass of Forms of RPA in Solution

	solution molecular mass (kDa)			
	RPA		70ΔC442	
species	0.1 M	1.5 M	0.1 M	1.5 M
human	115 ± 3.0	123 ± 9.9		
S. cerevisiae	101 ± 7.4	96 ± 8.8	37 ± 1.9	39 ± 1.7

It has been reported previously that RPA can aggregate at high protein concentrations (*47*) or in buffers of high ionic strength (*54*). Since aggregation will perturb the analysis of binding data, we identified solution conditions under which no aggregation occurred. An initial screen of solution conditions was carried out by incubating hRPA or scRPA at 25 °C and then subjecting the RPA to centrifugation in a microcentrifuge (10000*g*, 5 min). A decrease in RPA concentration monitored by intrinsic RPA fluorescence or UV absorbance (A = 280 nm) indicated aggregation. When 0.01% Tween 20 was added to standard buffers, no loss of RPA was observed at a variety of protein concentrations (43−200 nM and 5 μM) even after several hours of incubation at 25 °C (data not shown). To confirm these data and to determine whether these conditions had any effect on the solution state of hRPA or scRPA, the solution molecular mass was determined by equilibrium sedimentation. Under these conditions, both hRPA and scRPA were present in solution as single species with masses consistent with 1:1:1 heterotrimers (Table 1). In addition, velocity sedimentation and gel-permeation chromatography confirmed that recombinant scRPA had hydrodynamic parameters (S = 5.5 ± 1.5, Stokes radius = 47 ± 2 Å, calculated molecular mass = 108 kDa) similar to those published for the native enzyme (*49*). We conclude that in the presence of 0.01% Tween 20 both hRPA and scRPA are heterotrimers in solution and that under these conditions no aggregation occurs.

General Binding Properties of scRPA. Previously it has been shown that binding of both human and yeast RPA to ssDNA can be examined in gel mobility shift assays (GMSA) (*46*). The number of complexes formed with an oligonucleotide will depend on the affinity of the protein for the oligonucleotide and the occluded binding site size of the protein. Oligothymidine, 30 nucleotides in length [$(dT)_{30}$], was titrated with either hRPA or scRPA and the resulting complexes were analyzed on an agarose gel. With both proteins only a single band with altered mobility was observed and similar concentrations of each protein were needed to produce an RPA−ssDNA complex (Figure 1A). When similar assays were carried out with $(dT)_{50}$, two

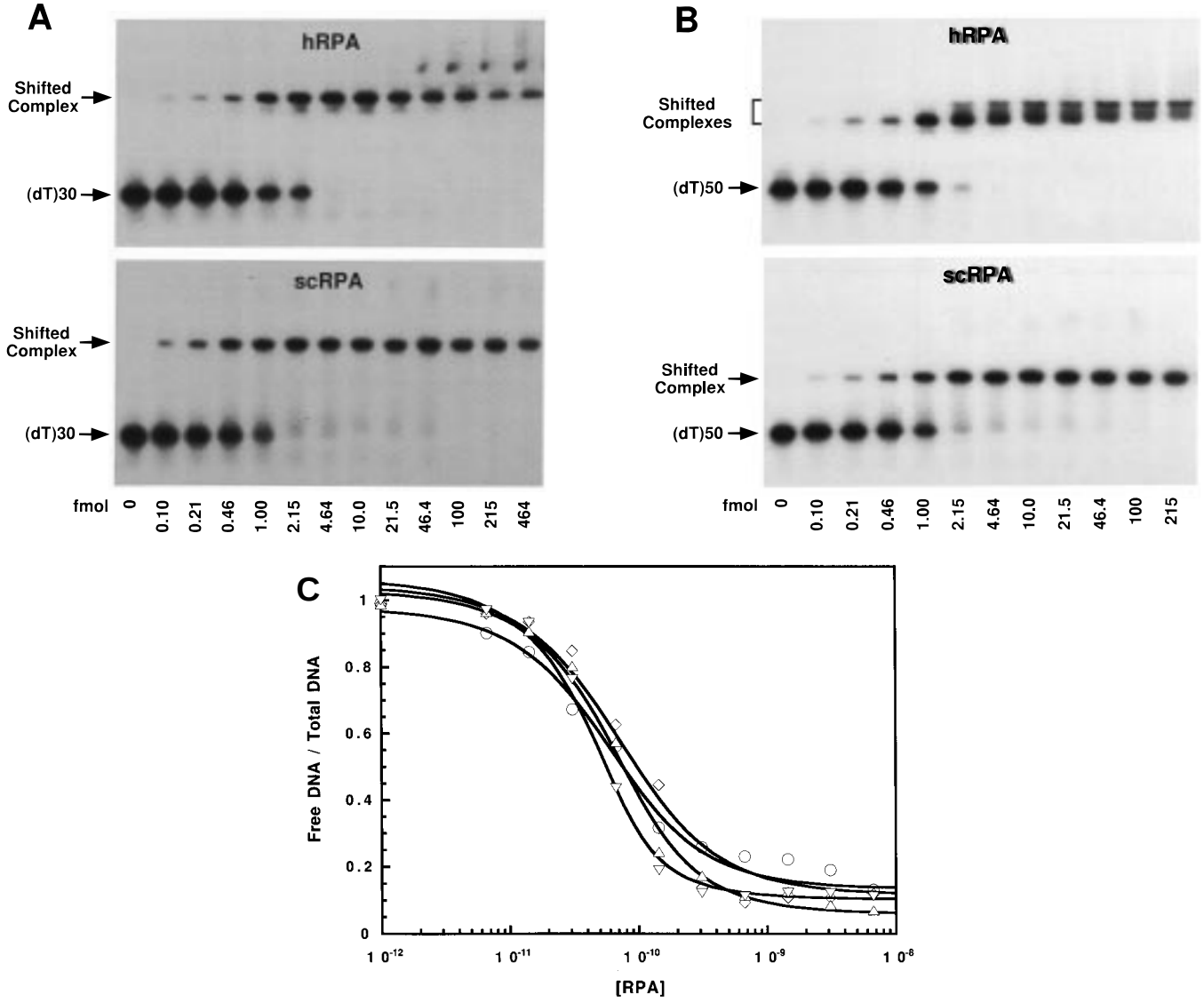

FIGURE 1: Gel mobility shift assay of hRPA and scRPA protein using radiolabeled oligonucleotides. Binding reactions (15 μL) were carried out with the indicated amounts of hRPA or scRPA protein in filter binding buffer. The protein was incubated at 25 °C for 20 min with 2 fmol of radiolabeled (A) $(dT)_{30}$ or (B) $(dT)_{50}$. The reaction mixtures were separated on a 1% agarose gel in 0.1× Tris acetate/EDTA (TAE) running buffer and analyzed as described in Experimental Procedures. The position of the shifted complexes and free oligonucleotide DNA are indicated. (C) Radioactivity present in free DNA and protein−DNA complexes in the gels shown in panels A and B was quantitated and the ratio of free DNA to total DNA was determined. These data were then plotted and fit to the Langmuir binding equation. Binding constants determined are shown in Table 3. (○) scRPA with $(dT)_{30}$; (◇) hRPA with $(dT)_{30}$; (△) scRPA with $(dT)_{50}$; (▽) hRPA with $(dT)_{50}$. Solid lines indicate best-fit curves. Span and minimum of data from hRPA with $(dT)_{50}$ was normalized to the other three data sets.

complexes with slower mobility were observed as increasing amounts of hRPA bound (Figure 1B). These two complexes represent singly and doubly liganded DNA, and their formation is consistent with the 30 nt occluded binding site observed previously for hRPA (*47*). In contrast, when scRPA was incubated with $(dT)_{50}$, only one shifted band with altered mobility was seen (Figure 1B). Similar results were observed at 10 times higher concentrations of scRPA (data not shown). When binding to $(dT)_{70}$ was examined, up to three complexes with altered mobility were observed with hRPA while a maximum of two complexes were observed with scRPA (data not shown; see also ref *47*). These data suggested that hRPA and scRPA have different occluded binding site sizes. However, these data were not consistent with an occluded binding site of 90−100 nt as reported previously for scRPA (*49*). If this were the case, multiple complexes should not have been observed with $(dT)_{70}$. Binding to a 295 nt oligonucleotide was also examined. Both hRPA and scRPA formed multiple complexes with the 295 nt oligonucleotide (Figure 2). The overall pattern of complexes observed with scRPA was similar but not identical to that of hRPA. This would not be the case if the occluded binding site sizes of hRPA and scRPA were 30 and 90 nt, respectively. The data shown in Figure 2 also provided information about the cooperativity of binding of scRPA. In the titrations shown in Figure 2, multiple partially saturated complexes with intermediate mobility were observed. However, if scRPA bound ssDNA with high cooperativity as initially reported (*49*), only free and fully saturated DNA should have been observed (*67*). These data indicate that scRPA binds with a cooperativity similar to that of hRPA. Similar patters were also observed when binding of hRPA or scRPA to M13 ssDNA was examined (data not shown). Preliminary quantitative analysis also indicated that the

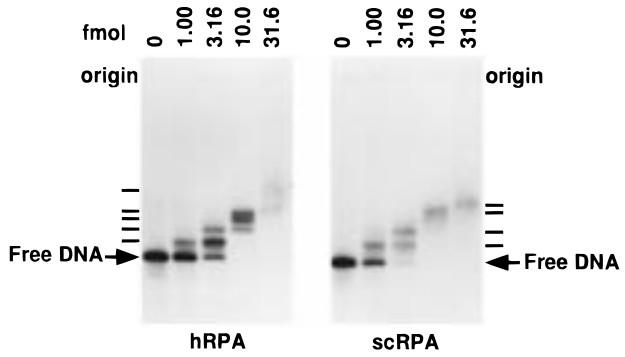

FIGURE 2: Gel mobility shift assay of hRPA and scRPA using long ssDNA. A 295 bp fragment containing the *Hin*dIII−*Sph*I SV40 origin DNA was amplified by PCR from pUC·HSO (*73*) using M13 forward and reverse primers. The resulting DNA fragment was isolated using a GenElute agarose spin column, treated with calf intestinal phosphatase, and radiolabeled using polynucleotide kinase. The radiolabeled fragment (1 fmol) was denatured at 100 °C, chilled to 0 °C, and mixed with the indicated amounts of hRPA or scRPA. After incubation at 25 °C for 20 min, the reaction mixtures were separated on a 1% agarose gel in 0.1× Tris acetate/EDTA (TAE) running buffer and analyzed as described in Experimental Procedures. The position of the gel origin (origin), shifted complexes (dashes), and free DNA (arrow) are indicated.

Table 2: Occluded Binding Site Size of RPA and RPA70ΔC442

	site size[a] (nt)	
species	RPA	RPA70ΔC442
human	34 ± 4	30 ± 5
S. cerevisiae	45 ± 3	31 ± 3

[a] Calculations were carried out as described in Experimental Procedures.

cooperativity parameters of hRPA and scRPA are very similar and of low magnitude (data not shown). We conclude that scRPA binds to ssDNA with low cooperativity and with an occluded binding site that is greater than that of hRPA but much less than 90 nt.

Quantitation of scRPA Binding Parameters. To reconcile the inconsistencies between published binding properties of scRPA (*49*, *57*) and those described above, a quantitative comparison of yeast and human RPA was carried out. Both hRPA and scRPA have an intrinsic fluorescence that decreases upon binding to ssDNA (*47*−*49*). When RPA is titrated with long ssDNA under stoichiometric binding conditions, saturation occurs when all of the protein is complexed with DNA. Thus, the saturation point is diagnostic of the occluded binding site size. A series of reverse titrations were carried out with hRPA or scRPA binding to poly(dT) under low-salt (stoichiometric binding) conditions. The occluded binding site determined for hRPA was 34 nt (Table 2); this value is in agreement with previous studies of hRPA (*46*, *47*) and quantitative studies of *Drosophila* and bovine RPA homologues (*54*, *56*). In contrast, under the same conditions the occluded binding site size of scRPA was 45 nt, 30% larger (Table 2). [Note the occluded binding site of a protein reflects the number of nucleotides that are covered when it binds to DNA. This parameter does not provide any information about the number of nucleotides that are interacting with RPA (the interaction site). Previous studies indicate that the high-affinity DNA-binding domain of RPA is the principal determiniant directing RPA binding and only interacts with ∼8 nucleotides (*15*, *20*, *24*, *25*)].

The data from GMSA titrations shown in Figure 1A,B was quantitated and apparent binding constants were determined by fitting the resulting binding isotherms to the Langmuir equation (see Figure 1C). Binding constants were also determined for both homologues of RPA using several oligonucleotides of lengths approximately equal to the occluded binding site size (Table 3). When hRPA or scRPA bound to $(dT)_{30}$, $(dT)_{50}$, or an oligonucleotide of mixed sequence $[(dGACT)_{7.5}]$, both RPA homologues had apparent association constants of approximately 1.0×10^{10} M^{-1} (Table 3). Since the DNA concentration used in these assays (∼0.1 nM) is approximately equal to the apparent association constant, binding was probably occurring under stoichiometric and not equilibrium conditions. This means that these apparent association constants must be considered lower limit estimates of the true equilibrium binding constants.

To obtain equilibrium binding constants for hRPA and scRPA, binding was also quantitated by fluorescence quenching. Previous studies have shown that the intrinsic fluorescence of both hRPA and scRPA is decreased (quenched) when bound to ssDNA (*47*, *48*; see also ref *65*). Fluorescence quenching directly monitors binding, and because no electrophoresis is required, the ionic strength present can be increased so that binding occurs under equilibrium conditions (*65*, *68*). Thus, while binding constants obtained from fluorescence studies cannot be directly compared to those obtained in GMSA because of differences in ionic strength between the assays, the relative binding affinities from both assays can be compared and should be consistent (see also ref *9*). To ensure that the solution structure of RPA was not changed by the high ionic strength used in fluorescence assays, the solution structure of both homologues was determined in the presence of 1.5 M NaCl by equilibrium centrifugation (Table 1). Neither aggregation nor multimerization was observed; both proteins remained heterotrimeric at 1.5 M NaCl.

Titrations of hRPA and scRPA were carried out with various oligonucleotides and the changes in fluorescence monitored. Ionic strength was varied until equilibrium binding was observed. Representative titrations with $(dT)_{30}$ are shown for both homologues in Figure 3. Binding constants were determined for hRPA and scRPA. scRPA had an association constant at least 5 times higher than that of hRPA with both $(dT)_{30}$ and $(dT)_{40}$ (Table 4). The affinity of scRPA for oligonucleotides of mixed sequence was 2 times higher than that of hRPA, while hRPA and scRPA had similar affinities for $(dA)_{30}$ (Table 4). We conclude that scRPA has a higher affinity for oligothymidine than does hRPA.

Comparison of the High-Affinity ssDNA-Binding Domain of Yeast and Human RPA. The experiments described above indicate that yeast and human RPA have different ssDNA binding properties. To determine the region(s) of RPA responsible for causing these different binding properties, we examined the DNA binding of fragments of RPA70 that contain the high-affinity ssDNA binding domain. The high-affinity ssDNA-binding domain is localized to the central domain of RPA70 in both human and yeast RPA (*9*, *15*, *69*). Previously we have shown that a fragment of hRPA70 made up of residues 1−441 (hRPA70ΔC442) is a monomer in solution, contains the entire ssDNA-binding domain, and binds ssDNA with an affinity that is approximately 1 order

Table 3: Binding Properties of hRPA and scRPA Determined by GMSA[a]

	apparent K_A ($\times 10^{-8}$ M^{-1})				
template	hRPA	scRPA	hRPA32·14	scRPA32·14	hRPA32core·14
$(dT)_{12}$	nd	nd	nd	NC	nd
$(dT)_{20}$	nd	nd	nd	0.034 ± 0.005	nd
$(dT)_{30}$	$\geq 130 \pm 50$ (S)	$\geq 150 \pm 40$ (S)	NC[b]	0.41 ± 0.08	$\geq 0.003 \pm 0.0005$
$(dT)_{50}$	$\geq 260 \pm 160$ (S)	$\geq 140 \pm 80$ (S)	nd	nd	nd
$(dGACT)_{7.5}$	$\geq 110 \pm 20$ (S)	$\geq 130 \pm 30$ (S)	NC	0.14 ± 0.04	nd

[a] S, stoichiometric or near-stoichiometric binding conditions (values represent the lower limit for association constant); NC, no complex observed; nd, not determined. [b] See also Figure 4.

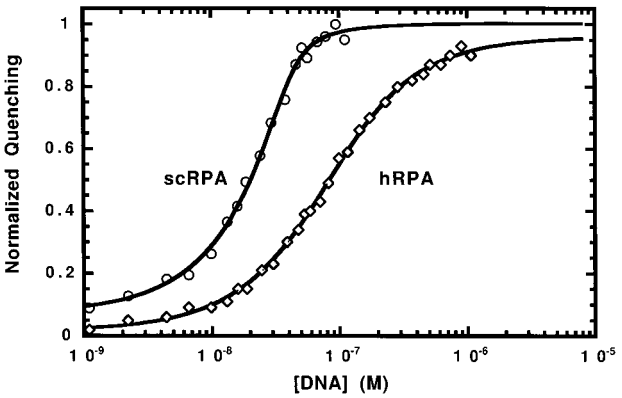

FIGURE 3: Binding of hRPA and scRPA to $(dT)_{30}$ monitored by fluorescence. hRPA (◇) and scRPA (○) (61and 40 nM active protein, respectively) were titrated with increasing amounts of $(dT)_{30}$ in 1× filter binding buffer in the presence of 0.01% Tween and 1.5 M NaCl at 25 °C. The absolute decrease (quenching) of the intrinsic fluorescent signal was plotted versus the DNA (molar) concentration. Quenching data was normalized prior to plotting; maximum quenching for hRPA and scRPA were 51% and 39%, respectively. Data were fitted to the Langmuir binding equation, and solid lines indicate best-fit curves. Binding constants determined are shown in Table 4. (Note that the binding curve for scRPA has the asymmetrical shape characteristic of stoichiometric binding conditions.)

of magnitude lower than that of the hRPA complex (*70*). A similar deletion containing residues 1−441 from scRPA70 was made (see Experimental Procedures) and shown to be monomeric in solution by analytical ultracentrifugation (Table 1). Binding of hRPA70ΔC442 and scRPA70ΔC442 to oligonucleotides was examined by fluorescence titration. Titrations of hRPA70ΔC442 and scRPA70ΔC442 did not saturate at 1.5 M NaCl, so binding constants were determined at 1 M NaCl where binding was saturable (data not shown). This indicates that hRPA70ΔC442 and scRPA70ΔC442 have a lower affinity for ssDNA than heterotrimeric RPA. hRPA70ΔC442 and scRPA70ΔC442 bound ssDNA with similar affinities; the largest difference observed between these two fragments was a 2-fold difference in affinity for $(dT)_{30}$ (Table 4). We conclude that the high-affinity binding domain in RPA70 is not responsible for the observed differences in DNA binding between these two homologues. In addition, the occluded binding sites for hRPA70ΔC442 and scRPA70ΔC442 were identical; both are approximately 31 nt (Table 2). This site size is close to that of hRPA indicating that the occluded binding site size for hRPA is primarily determined by the 70-kDa subunit. In contrast, the binding site size of scRPA70ΔC442 is 14 nt smaller than that of scRPA, indicating that additional regions of scRPA are probably interacting with ssDNA.

Binding of the RPA32·14 Subcomplex to ssDNA. The 32-kDa subunit of both hRPA and scRPA has weak ssDNA binding activity (*15*, *34*−*36*). However, while these data suggest that this subunit can interact with ssDNA, no quantitative analysis of this interaction has been carried out. In addition, there has been no direct comparison of the 32-kDa subunits from human and yeast RPA.

We examined the DNA-binding properties of subcomplexes containing the 32-kDa and 14-kDa subunits of yeast and human RPA, scRPA32·14 and hRPA32·14, respectively. When $(dT)_{50}$ was titrated with scRPA32·14 and the products were separated on an agarose gel, a single complex with slower mobility was observed (Figure 4B). Similar data were obtained with $(dT)_{30}$ and $(dGACT)_{7.5}$ (data not shown). These binding data were quantitated, binding isotherms were generated, and apparent binding constants were determined. scRPA32·14 binds to ssDNA with an affinity at least 3 orders of magnitude lower than that of the heterotrimeric scRPA complex (compare binding constants for scRPA32·14 with those of hRPA and scRPA; Table 3). Furthermore, the affinity for $(dT)_{30}$ was 4-fold higher than for a 30-mer of mixed sequence (Table 3). In contrast to scRPA32·14, no complex with altered mobility was seen for hRPA32·14, even at high protein concentrations (Figure 4A). These results agree with previous studies of the hRPA32·14 subcomplex (*26*). Several preparations of hRPA32·14 were assayed, including a His-tagged complex that was purified by nickel affinity chromatography. Identical results were obtained with all hRPA32·14 preparations (data not shown). These data indicate either that hRPA32·14 is unable to bind to ssDNA or that it binds with an affinity much lower than the yeast subcomplex. To distinguish between these possibilities, we reexamined binding with 10-fold higher concentrations of $(dT)_{30}$ and 1000-fold higher concentrations of hRPA32·14. Under these conditions, a single band with altered mobility was observed (Figure 4C). There was no change in the mobility of the DNA when identical amounts of other, non-DNA-binding proteins (such as bovine serum albumin) were used (data not shown). Therefore, we believe that the complex observed in Figure 4C is caused by direct interactions between hRPA32·14 and ssDNA; however, because of the high level of protein required for this interaction, we cannot rule out that the complex is caused by a low-level contaminant. These results indicate that the RPA32·14 subcomplexes from both human and *S. cerevisiae* interact with ssDNA and that the affinity of the *S. cerevisiae* subcomplex is more than 1000-fold greater than that of the human subcomplex.

Bochkareva et al. (*36*) have characterized the DNA-binding activity of hRPA32·14 complexes containing mutant

Table 4: Binding Properties of hRPA and scRPA Determined by Fluorescence[a]

		apparent K_A ($\times 10^{-6}$ M^{-1})			
template	[NaCl] (M)	hRPA	scRPA	h70ΔC442	sc70ΔC442
$(dA)_{30}$	0.5	31 ± 6	43 ± 9	nd	nd
$(dT)_{30}$	1.0	nd	nd	1.5 ± 0.2	3.2 ± 0.5
	1.5	39 ± 13	≥220 ± 68 (S)	NS	NS
$(dT)_{40}$	1.0	nd	nd	nd	4.4 ± 1.2
	1.5	34 ± 2	≥140 ± 32 (S)	nd	NS
$(dGACT)_{7.5}$	0.5	nd	nd	1.5 ± 0.2	1.9 ± 0.2
	1.5	15 ± 1	26 ± 2	NS	NS
$(dGACT)_{10}$	1.5	6 ± 0.2	12 ± 0.8	nd	nd

[a] Concentrations of hRPA and scRPA used in fluorescence assays ranged from 14 to 58 nM and from 27 to 40 nM, respectively. S, stoichiometric or near-stoichiometric binding conditions (values represent the lower limit for association constant); NS, not possible to saturate binding; nd, not determined.

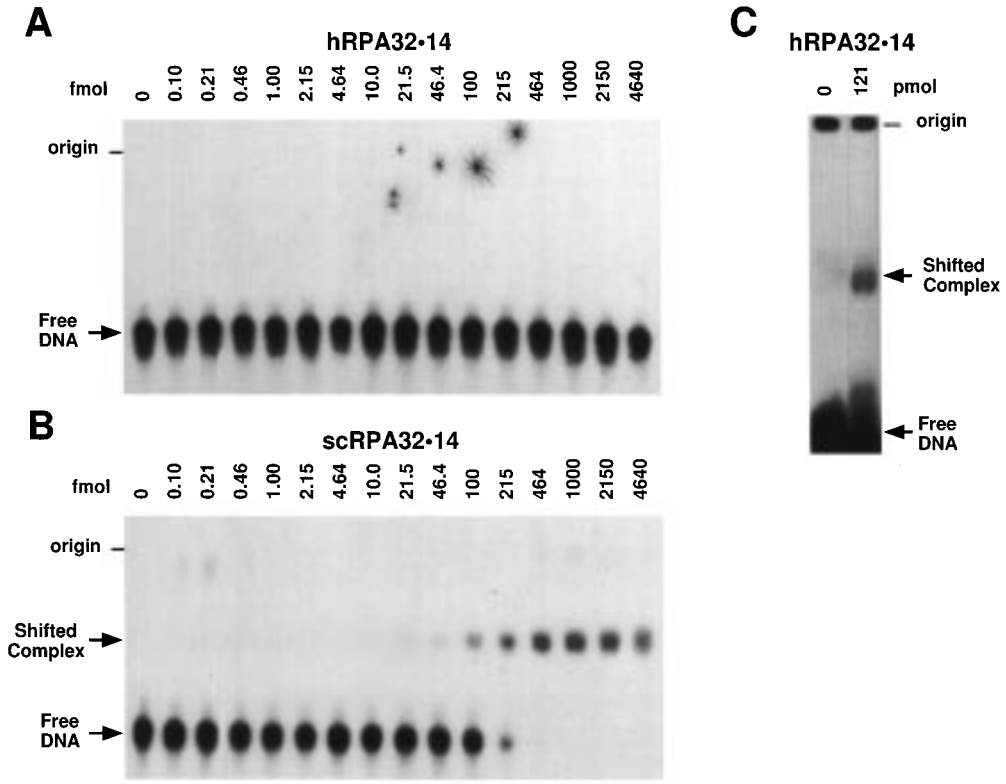

FIGURE 4: Gel mobility shift assay of hRPA32·14 and scRPA32·14 subcomplexes using radiolabeled oligonucleotides. Radiolabeled $(dT)_{50}$ (2 fmol) was incubated with the indicated amounts of hRPA32·14 subcomplex (A) or scRPA32·14 subcomplex (B) for 20 min at 25 °C in filter binding buffer. (C) Radiolabeled $(dT)_{30}$ (20 fmol) was incubated with the indicated amounts of hRPA32·14 subcomplex (picomoles) for 20 min at 25 °C in a total volume of 15 μL containing 25 mM HEPES (diluted from a 1 M stock, pH 7.8), 200 mM NaCl, 4% glycerol, 0.5 mM dithiothreitol, and 0.l% Nonidet 40. Reaction mixtures were separated on a 1% agarose gel in 0.1× Tris acetate/EDTA (TAE) running buffer and analyzed as described in Experimental Procedures. The positions of the gel origin (origin), shifted complexes, and free DNA are indicated.

forms of hRPA32. They showed that a complex containing only the core domain of hRPA32, residues 43−171, has a higher affinity for ssDNA than does a complex with full-length RPA32. We wanted to determine how this higher affinity subcomplex of hRPA compared to scRPA32·14. A subcomplex containing the core of hRP32 and hRPA14 [hRPA32(43−171)·14] was purified and assayed for binding for ssDNA binding activity. hRPA32(43−171)·14 bound ssDNA with an affinity higher than hRPA32·14 (data not shown). However, the association constant of hRPA32(43−171)·14 was less than $^1/_{100}$ that of scRPA32·14 (Table 3). We conclude that deletion of the N- and C-terminal domains of hRPA32 does not expose a high-affinity ssDNA-binding domain and that the DNA-binding activity of hRPA32 is intrinsically much less than that of scRPA32.

The binding of scRPA32·14 to oligonucleotides of different lengths was also examined. As the length of the oligonucleotide was decreased, the association constant of scRPA32·14 also decreased: the affinity for $(dT)_{20}$ was approximately $^1/_{10}$ that for $(dT)_{30}$ and no binding was detected with $(dT)_{12}$ (Table 3).

DISCUSSION

We determined the DNA binding parameters for both hRPA and scRPA. These studies are the first direct comparison of these proteins under identical conditions. We find that hRPA and scRPA have different binding parameters. Both RPA homologues bind ssDNA with high affinity and low cooperativity. However, scRPA has an occluded binding site 11 nt larger and a 5-fold higher affinity for oligothy-

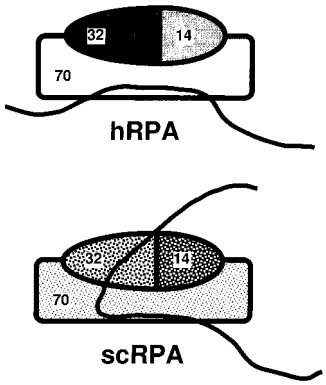

FIGURE 5: Schematic of hypothetical ssDNA binding modes of human and yeast RPA. Hypothetical binding modes for hRPA and scRPA are shown. DNA (solid line) binds predominantly to the high-affinity DNA-binding domain of hRPA70 and binds both to the high-affinity DNA-binding domain of scRPA70 and to scRPA32. See text for details.

midine than hRPA. Taken together, these data indicate that scRPA and hRPA have different modes of binding to ssDNA.

We localized the cause of the difference in binding activities to the 32, and 14-kDa subunits. Deletion mutants of RPA70 containing the entire high-affinity ssDNA-binding domain (hRPA70ΔC442 and scRPA70ΔC442) were shown to have identical DNA-binding properties, while subcomplexes of scRPA32·14 and hRPA32·14 had distinctly different DNA-binding properties. scRPA32·14 had a preference for binding oligothymidine and had an affinity for ssDNA more than 1000-fold higher than that of hRPA32·14 (Table 2). Thus, we propose that direct interactions between scRPA32·14 and ssDNA are causing scRPA to have a higher affinity for oligothymidine and a larger occluded binding site size than hRPA. These extra interactions make it likely that ssDNA wraps around scRPA when bound (Figure 5). This conclusion is supported by previous studies that visualized RPA·DNA complexes using electron microscopy. In these independent studies, hRPA formed linear arrays with ssDNA and caused a minimal decrease in the length of the DNA suggesting that the DNA was bound along one face of the protein (49), while scRPA formed nucleosomelike structures, suggesting that the DNA was wrapped around the protein (*71*). (However, it should be noted that these two studies were carried out independently and may not be directly comparable.)

Our results contradict the one previous quantitative study of scRPA DNA-binding properties, which concluded that scRPA bound with very high cooperativity and had an occluded binding site size of 90−100 nt (*49*). This discrepancy is probably not caused by differences between native (used in ref *49*) and recombinant RPA (used in these studies) because we have observed that native and recombinant scRPA have similar DNA-binding properties (data not shown). Nor can this discrepancy be explained by differences in assay conditions because we have observed identical DNA-binding properties under the assay conditions used in the previous study (data not shown) and hRPA has been found to have similar binding properties under a wide range of solution conditions (*47, 48*). It also is unlikely that differences in the posttranslational modification state such as phosphorylation are the source of the discrepancy. RPA purified from HeLa or yeast cells is usually unphosphorylated and we find no detectable phosphorylation of native scRPA characterized in our laboratory (data not shown). We feel that it is most likely that the discrepancy between the values determined here and those reported previously was caused by the difficulty in defining the binding parameters of ssDNA-binding proteins. The binding parameters of cooperativity, intrinsic binding constant, and occluded binding site size are very tightly correlated so it is difficult to resolve all three parameters unambiguously (*68*). We have found that if all three parameters are fit simultaneously, a wide range of values for cooperativity, occluded binding site size, and binding affinity can describe a single RPA binding isotherm. Without constraining at least one parameter by independent determination (e.g., binding site size), it is impossible to distinguish which set of parameters best describe the binding reaction. It seems likely that the high cooperativity and large binding site size reported previously represent one of these alternate sets of parameters that does not reflect the true binding properties of scRPA.

All mutant forms of RPA that are missing the C-terminus of RPA70 and 32- and 14-kDa subunits have reduced affinity for ssDNA (*9, 21*−*24*). In the case of hRPA70ΔC442, this reduction is approximately an order of magnitude (*9, 21*). These data suggest that either the C-terminus of RPA70 or the 32- and 14-kDa subunits of hRPA may be contributing approximately 1 order of magnitude to the overall affinity of the hRPA complex for ssDNA. This increase in affinity could be caused either by weak interactions of hRPA32 with DNA or by effects on the structure of the high-affinity ssDNA-binding domain. There are multiple precedents for weak binding sites becoming very significant physiologically when coupled with stronger binding sites (*72*).

The crystal structure of the DNA-binding domain of the 70-kDa subunit indicates that it is composed of two copies of a conserved ssDNA-binding motifs and that the binding domain interacts with 8 nt of DNA (*25*). Each of the ssDNA-binding motifs interacts with ∼4 nt (*25*). On the basis of DNA sequence, RPA32 contains a single ssDNA-binding motif (*15*). Thus, RPA32·14 should have an interaction site of approximately 4 nt. In this case, scRPA32·14 would be expected to have a similar affinity for short oligonucleotides of different lengths. Instead a strong length dependence of binding was observed (Table 3). Moreover, the observed length dependence is greater than would be predicted by the increased number of possible binding sites present on the longer oligonucleotides. This suggests that there is some form of cooperativity in scRPA32·14 binding. Either there are multiple sites in scRPA32·14 interacting with ssDNA or scRPA32·14 binds as a dimer. Both of these possibilities would make the effective binding site larger and thus could cause the observed length dependence of binding.

It has been recently shown that the core domain of hRPA32 binds to ssDNA with a higher affinity than full-length hRPA32 (36). However, even a subcomplex containing hRPA32(43−171)·14 binds to ssDNA with an affinity less than $^1/_{100}$ that of scRPA32·14. Thus the DNA-binding activity of hRPA32 is intrinsically much weaker than that of scRPA32.

Two recent studies have shown that hRPA32 can be cross-linked to nascent DNA (*34, 35*). This raises the possibility that during DNA replication the 70-kDa subunit interacts with the template strand and the 32-kDa subunit interacts

with the nascent strand. If this is the case, RPA may have an active role coordinating reactions between the template and nascent strands at the replication fork or between two strands of DNA during DNA repair or recombination.

RPA homologues from different organisms are not functionally equivalent. The differences in function have been previously attributed to differences in the ability of different RPA homologues to participate in specific protein−protein interactions (*37*−*40*, *44*, *45*). In this paper, we show that hRPA and scRPA have different modes of binding to ssDNA. We suggest that this difference may also contribute to differences in functional activity between RPA homologues. Additional studies will be needed to determine the relative contributions of RPA−protein and RPA−DNA interactions to RPA function.

ACKNOWLEDGMENT

We thank M. Bjerke and P. Lashmit for initial subcloning of yeast RPA genes. We thank L. A. Henricksen and P. Burgers for supplying purified recombinant hRPA and native scRPA, respectively, and we thank L. A. Henricksen and A. P. Walther for purified hRPA32•14 subcomplex. We thank the members of the Wold laboratory for scientific discussions and critical reading of the manuscript. We also thank Aled Edwards, Gabriel Kauffman, and Olga Lavrik for sharing their results prior to publication. We thank the University of Iowa DNA Core Facility for oligonucleotide synthesis and DNA sequencing.

REFERENCES

1. Wobbe, C. R., Weissbach, L., Borowiec, J. A., Dean, F. B., Murakami, Y., Bullock, P., and Hurwitz, J. (1987) *Proc. Natl. Acad. Sci. U.S.A. 84*, 1834−1838.
2. Wold, M. S., and Kelly, T. (1988) *Proc. Natl. Acad. Sci. U.S.A. 85*, 2523−2527.
3. Fairman, M. P., and Stillman, B. (1988) *EMBO J. 7*, 1211−1218.
4. Wold, M. S. (1997) *Annu. Rev. Biochem. 66*, 61−92.
5. Longhese, M. P., Neecke, H., Paciotti, V., Lucchini, G., and Plevani, P. (1996) *Nucleic Acids Res. 24*, 3533−3537.
6. Brush, G. S., Morrow, D. M., Hieter, P., and Kelly, T. J. (1996) *Proc. Natl. Acad. Sci. U.S.A. 93*, 15075−15080.
7. Miller, S. D., Moses, K., Jayaraman, L., and Prives, C. (1997) *Mol. Cell. Biol. 17*, 2194−2201.
8. Van der Knaap, E., Jagoueix, S., and Kende, H. (1997) *Proc. Natl. Acad. Sci. U.S.A. 94*, 9979−9983.
9. Gomes, X. V., and Wold, M. S. (1996) *Biochemistry 35*, 10558−10568.
10. Heyer, W.-D., Rao, M. R. S., Erdile, L. F., Kelly, T. J., and Kolodner, R. D. (1990) *EMBO J. 9*, 2321−2329.
11. Brill, S. J., and Stillman, B. (1991) *Genes Dev. 5*, 1589−1600.
12. Smith, J., and Rothstein, R. (1995) *Mol. Cell. Biol. 15*, 1632−1641.
13. Firmenich, A. A., Elias-Arnanz, M., and Berg, P. (1995) *Mol. Cell. Biol. 15*, 1620−1631.
14. Longhese, M. P., Plevani, P., and Lucchini, G. (1994) *Mol. Cell. Biol. 14*, 7884−7890.
15. Philipova, D., Mullen, J. R., Maniar, H. S., Gu, C., and Brill, S. J. (1996) *Genes Dev. 10*, 2222−2233.
16. Maniar, H. S., Wilson, R., and Brill, S. J. (1997) *Genetics 145*, 891−902.
17. Santocanale, C., Neecke, H., Longhese, M. P., Lucchini, G., and Plevani, P. (1995) *J. Mol. Biol. 254*, 595−607.
18. Parker, A. E., Clyne, R. K., Carr, A. M., and Kelly, T. J. (1997) *Mol. Cell. Biol. 17*, 2381−2390.
19. Reference deleted in proof.
20. Gomes, X. V., Henricksen, L. A., and Wold, M. S. (1996) *Biochemistry 35*, 5586−5595.
21. Gomes, X. V., and Wold, M. S. (1995) *J. Biol. Chem. 270*, 4534−4543.
22. Kim, D. K., Stigger, E., and Lee, S. H. (1996) *J. Biol. Chem. 271*, 15124−15129.
23. Lin, Y. L., Chen, C., Keshav, K. F., Winchester, E., and Dutta, A. (1996) *J. Biol. Chem. 271*, 17190−17198.
24. Pfuetzner, R. A., Bochkarev, A., Frappier, L., and Edwards, A. M. (1997) *J. Biol. Chem. 272*, 430−434.
25. Bochkarev, A., Pfuetzner, R. A., Edwards, A. M., and Frappier, L. (1997) *Nature 385*, 176−181.
26. Henricksen, L. A., Umbricht, C. B., and Wold, M. S. (1994) *J. Biol. Chem. 269*, 11121−11132.
27. Lee, S.-H., and Kim, D. K. (1995) *J. Biol. Chem. 270*, 12801−12807.
28. Nagelhus, T. A., Haug, T., Singh, K. K., Keshav, K. F., Skorpen, F., Otterlei, M., Bharati, S., Lindmo, T., Benichou, S., Benarous, R., and Krokan, H. E. (1997) *J. Biol. Chem. 272*, 6561−6566.
29. Saijo, M., Kuraoka, I., Masutani, C., Hanaoka, F., and Tanaka, K. (1996) *Nucleic Acids Res. 24*, 4719−4724.
30. Din, S.-U., Brill, S. J., Fairman, M. P., and Stillman, B. (1990) *Genes Dev. 4*, 968−977.
31. Dutta, A., Ruppert, J. M., Aster, J. C., and Winchester, E. (1993) *Nature 365*, 79−82.
32. Blackwell, L. J., Borowiec, J. A., and Mastrangelo, I. A. (1996) *Mol. Cell Biol. 16*, 4798−4807.
33. Niu, H. W., Erdjument-Bromage, H., Pan, Z. Q., Lee, S. H., Tempst, P., and Hurwitz, J. (1997) *J. Biol. Chem. 272*, 12634−12641.
34. Lavrik, O. I., Nasheuer, H. P., Weisshart, K., Wold, M. S., Prasad, R., Beard, W. A., Wilson, S. H., and Favre, A. (1998) *Nucleic Acids Res. 26*, 602−607.
35. Mass, G., Nethanel, T., and Kaufmann, G. (1998) *Mol. Cell. Biol.* (in press).
36. Bochkareva, E., Frappier, L., Edwards, A. M., and Bochkarev, A. (1998) *J. Biol. Chem. 273*, 3932−3936.
37. Braun, K. A., Lao, Y., He, Z., Ingles, C. J., and Wold, M. S. (1997) *Biochemistry 36*, 8443−8454.
38. Nasheuer, H. P., von Winkler, D., Schneider, C., Dornreiter, I., Gilbert, I., and Fanning, E. (1992) *Chromosoma 102*, S52−S59.
39. Kamakaka, R. T., Kaufman, P. D., Stillman, B., Mitsis, P. G., and Kadonaga, J. T. (1994) *Mol. Cell. Biol. 14*, 5114−5122.
40. Melendy, T., and Stillman, B. (1993) *J. Biol. Chem. 268*, 3389−3395.
41. Brown, G. W., Melendy, T., and Ray, D. S. (1993) *Mol. Biochem. Parasitol. 59*, 323−326.
42. Brown, G. W., Melendy, T. E., and Ray, D. S. (1992) *Proc. Natl. Acad. Sci. U.S.A. 89*, 10227−10231.
43. Ishiai, M., Sanchez, J. P., Amin, A. A., Murakami, Y., and Hurwitz, J. (1996) *J. Biol. Chem. 271*, 20868−20878.
44. Collins, K. L., and Kelly, T. J. (1991) *Mol. Cell. Biol. 11*, 2108−2115.
45. Dornreiter, I., Erdile, L. F., Gilbert, I. U., von Winkler, D., Kelly, T. J., and Fanning, E. (1992) *EMBO J. 11*, 769−776.
46. Kim, C., Snyder, R. O., and Wold, M. S. (1992) *Mol. Cell. Biol. 12*, 3050−3059.
47. Kim, C., Paulus, B. F., and Wold, M. S. (1994) *Biochemistry 33*, 14197−14206.
48. Kim, C., and Wold, M. S. (1995) *Biochemistry 34*, 2058−2064.
49. Alani, E., Thresher, R., Griffith, J. D., and Kolodner, R. D. (1992) *J. Mol. Biol. 227*, 54−71.
50. Wold, M. S., Weinberg, D. H., Virshup, D. M., Li, J. J., and Kelly, T. J. (1989) *J. Biol. Chem. 264*, 2801−2809.
51. Brill, S. J., and Stillman, B. (1989) *Nature 342*, 92−95.
52. Blackwell, L. J., and Borowiec, J. A. (1994) *Mol. Cell. Biol. 14*, 3993−4001.
53. Seroussi, E., and Lavi, S. (1993) *J. Biol. Chem. 268*, 7147−7154.

54. Mitsis, P. G., Kowalczykowski, S. C., and Lehman, I. R. (1993) *Biochemistry 32*, 5257−5266.
55. Marton, R. F., Thömmes, P., and Cotterill, S. (1994) *FEBS Lett. 342*, 139−144.
56. Atrazhev, A., Zhang, S., and Grosse, F. (1992) *Eur. J. Biochem. 210*, 855−865.
57. Sugiyama, T., Zaitseva, E. M., and Kowalczykowski, S. C. (1997) *J. Biol. Chem. 272*, 7940−7945.
58. Studier, F. W., Rosenberg, A. H., Dunn, J. J., and Dubendorff, J. W. (1990) *Methods Enzymol. 185*, 60−89.
59. Ausubel, F. M., Brent, R., Kingston, R. E., Moore, D. D., Seidman, J. G., Smith, J. A., and Struhl, K. (1989) in *Current protocols in molecular biology*, John Wiley and Sons, New York.
60. Pace, C. N., Vajdos, F., Fee, L., Grimsley, G., and Gray, T. (1995) *Protein Sci. 4*, 2411−2423.
61. Edelhoch, H. (1967) *Biochemistry 6*, 1948−1954.
62. Laue, T. M. (1995) *Methods Enzymol. 259*, 427−452.
63. Johnson, M. L., Correia, J. J., Yphantis, D. A., and Halvorson, H. R. (1981) *Biophys. J. 36*, 575−588.
64. Johnson, M. L., and Frasier, S. G. (1985) *Methods Enzymol. 117*, 301−342.
65. Lohman, T. M., and Mascotti, D. P. (1992) *Methods Enzymol. 212*, 424−458.
66. Ishiai, M., Sanchez, J. P., Amin, A. A., Murakami, Y., and Hurwitz, J. (1996) *J. Biol. Chem. 271*, 20868−20878.
67. Lohman, T. M., Bujalowski, W., and Overman, L. B. (1988) *Trends Biochem. Sci. 13*, 250−255.
68. Lohman, T. M., and Mascotti, D. P. (1992) *Methods Enzymol. 212*, 400−424.
69. Bochkarev, A., Pfuetzner, R. A., Edwards, A. M., and Frappier, L. (1997) *Nature 385*, 176−181.
70. Liao, S.-M., Zhang, J., Jeffery, D. A., Koleske, A. J., Thompson, C. M., Chao, D. M., Viljoen, M., Van Vuuren, H. J. J., and Young, R. A. (1995) *Nature 374*, 193−196.
71. Treuner, K., Ramsperger, U., and Knippers, R. (1996) *J. Mol. Biol. 259*, 104−112.
72. Ackers, G. K., Shea, M. A., and Smith, F. R. (1983) *J. Mol. Biol. 170*, 223−242.
73. Wold, M. S., Li, J. J., and Kelly, T. J. (1987) *Proc. Natl. Acad. Sci. U.S.A. 84*, 3643−3647.

BI981110+